Title

Enhanced phasic GABA inhibition during the repair phase of stroke: a novel therapeutic target

Journal

Brain, 139(2)

ISSN

0006-8950

Authors

Hiu, Takeshi
Farzampour, Zoya
Paz, Jeanne T
et al.

Publication Date

2016-02-01

DOI

10.1093/brain/awv360

doi:10.1093/brain/awv360 BRAIN 2016: 139; 468–480 | 468

BRAIN
A JOURNAL OF NEUROLOGY

Enhanced phasic GABA inhibition during the repair phase of stroke: a novel therapeutic target

Takeshi Hiu,[1,2,*] Zoya Farzampour,[3,*] Jeanne T. Paz,[3,4] Eric Hou Jen Wang,[1,2] Corrine Badgely,[3] Andrew Olson,[1] Kristina D. Micheva,[5] Gordon Wang,[5] Robin Lemmens,[1,2,6] Kevin V. Tran,[1,2] Yasuhiro Nishiyama,[1,2] Xibin Liang,[1,2] Scott A. Hamilton,[1,2] Nancy O'Rourke,[5] Stephen J. Smith,[5] John R. Huguenard,[3] Tonya M. Bliss[1,2,†] and Gary K. Steinberg[1,2,3,†]

*These authors contributed equally to this work.
†These authors are co-senior authors.

Ischaemic stroke is the leading cause of severe long-term disability yet lacks drug therapies that promote the repair phase of recovery. This repair phase of stroke occurs days to months after stroke onset and involves brain remapping and plasticity within the peri-infarct zone. Elucidating mechanisms that promote this plasticity is critical for the development of new therapeutics with a broad treatment window. Inhibiting tonic (extrasynaptic) GABA signalling during the repair phase was reported to enhance functional recovery in mice suggesting that GABA plays an important function in modulating brain repair. While tonic GABA appears to suppress brain repair after stroke, less is known about the role of phasic (synaptic) GABA during the repair phase. We observed an increase in postsynaptic phasic GABA signalling in mice within the peri-infarct cortex specific to layer 5; we found increased numbers of α1 receptor subunit-containing GABAergic synapses detected using array tomography, and an associated increased efficacy of spontaneous and miniature inhibitory postsynaptic currents in pyramidal neurons. Furthermore, we demonstrate that enhancing phasic GABA signalling using zolpidem, a Food and Drug Administration (FDA)-approved GABA-positive allosteric modulator, during the repair phase improved behavioural recovery. These data identify potentiation of phasic GABA signalling as a novel therapeutic strategy, indicate zolpidem's potential to improve recovery, and underscore the necessity to distinguish the role of tonic and phasic GABA signalling in stroke recovery.

1 Department of Neurosurgery, Stanford University, Stanford, CA, USA
2 Stanford Stroke Centre, Palo Alto, CA 94304, USA
3 Department of Neurology and Neurological Sciences, Stanford University, Stanford, CA, USA
4 Gladstone Institute of Neurological Disease and University of California, San Francisco San Francisco, CA USA
5 Department of Molecular and Cellular Physiology, Stanford University, Stanford, CA, USA
6 KU Leuven - University of Leuven, Department of Neurosciences, Experimental Neurology; VIB - Vesalius Research Centre University Hospitals Leuven, Department of Neurology, B-3000 Leuven, Belgium

Correspondence to: Tonya M. Bliss,
Department of Neurosurgery,
MSLS, p308, 1201 Welch Rd,
Stanford, CA 94035
E-mail: tbliss1@stanford.edu

Correspondence may also be addressed to: Gary K. Steinberg, Department of Neurosurgery, 300 Pasteur Drive, R301A, Stanford, CA 94305-5325. E-mail: gsteinberg@stanford.edu

Received May 11, 2015. Revised October 13, 2015. Accepted October 20, 2015. Advance Access publication December 18, 2015

Keywords: stroke; phasic GABA; brain repair; zolpidem

Abbreviations: $GABA_AR$ = GABA type A receptor; IPSC = postsynaptic inhibitory current

Introduction

Mechanisms that promote brain repair and recovery offer novel drug targets for stroke, a major cause of adult disability with very few therapeutic options. The majority of available treatments target the acute phase of ischaemic stroke to establish reperfusion and reduce brain cell death, but must be administered within a few hours of stroke onset (Allen *et al.*, 2012; Berkhemer *et al.*, 2015). Unfortunately, <10% of stroke patients can benefit from such treatments due, in large part, to late referral to the hospital and inability to meet other eligibility criteria (Allen *et al.*, 2012). In contrast to the acute stage, the repair phase of stroke occurs days to months after the stroke incident and thus offers an expanded therapeutic window. Importantly, brain plasticity and remapping during the repair phase play a major role in the spontaneous recovery observed after stroke in both humans and rodents. For example, reorganization and rewiring of surviving circuits, including those adjacent to the stroke site (i.e. the peri-infarct), enable the healthy portion of the brain to compensate for the functions of the stroke-damaged area (Nudo *et al.*, 1996; Dijkhuizen *et al.*, 2001; Carmichael, 2006; Murphy and Corbett, 2009). Deciphering the specific synaptic changes involved in the repair phase of stroke, and identifying those that can be modulated to improve outcome, is paramount to identifying novel therapeutics to promote functional recovery.

GABA type A receptor ($GABA_AR$)-mediated inhibition is a critical component in the development and plasticity of cortical map boundaries in the normal brain (Zheng and Knudsen, 2001; Derdikman *et al.*, 2003; Hensch and Stryker, 2004; Foeller *et al.*, 2005). The GABAergic signalling mechanisms that modulate cortical map boundaries in the normal brain may also mediate the stroke-induced cortical remapping required for functional recovery. Indeed, a role for GABA in plasticity-related recovery was suggested by Clarkson *et al.* (2010) who observed an increase tonic GABA signalling—a form of $GABA_AR$-mediated inhibition that relies on extrasynaptic $GABA_AR$'s—in the peri-infarct cortex during the repair phase (Clarkson *et al.*, 2010). These authors found that systemically reducing tonic GABA-mediated inhibition during this phase improved recovery, suggesting that the post-stroke increase in tonic inhibition is detrimental to recovery of function. Phasic GABA inhibition is the classical mode of GABA signalling mediated, largely, by $GABA_ARs$ at the synapse. While enhancing phasic GABA is known to be neuroprotective and reduce excitotoxic neuron death in the acute phase of stroke (Lyden and Hedges, 1992; Green *et al.*, 2000), its role in plasticity-related recovery during the repair phase of stroke is largely unknown. Specific $GABA_ARs$ mediate each form of GABA signalling, which renders phasic and tonic inhibition differentially susceptible to pharmacological manipulation. $GABA_ARs$ are heteropentameric proteins, with synaptic receptors generally consisting of two α, two β, and a γ subunit (Fritschy and Mohler, 1995). While multiple subunit isoforms have been identified (six α, four β, and three γ isoforms), $GABA_ARs$ containing the $\alpha 1$ subunit are the most highly expressed synaptic $GABA_AR$ in the mammalian brain and are thought to mediate the majority of phasic inhibition (Fritschy and Mohler, 1995). By contrast, tonic inhibition is mediated by distinct receptor heteromers containing either an $\alpha 5$ isoform or $\alpha 4$ isoform and a δ subunit substituted for γ (Farrant and Nusser, 2005).

Decreased expression of synaptic $GABA_AR$ subunits (Schiene *et al.*, 1996; Neumann-Haefelin *et al.*, 1998; Qu *et al.*, 1998; Redecker *et al.*, 2000; Jolkkonen *et al.*, 2003), combined with studies reporting decreased phasic GABA signalling in layer 2/3 pyramidal neurons at the onset of functional recovery (Neumann-Haefelin *et al.*, 1995; Clarkson *et al.*, 2010), suggest that phasic GABA signalling is reduced in the repair phase of stroke, but the significance of this for recovery is not known. Another study found no change in GABA signalling in layer 2/3 in the first 3 days after stroke (Mittmann *et al.*, 1998). Importantly, recent case reports demonstrate that treatment with zolpidem, an FDA-approved $GABA_A$ positive allosteric modulator with highest affinity for $\alpha 1$-containing receptors (Crestani *et al.*, 2000), improved brain function in patients with severe brain injuries, including stroke (Shames and Ring, 2008; Hall *et al.*, 2010). Although it is hard to extrapolate the involvement of phasic GABA in brain recovery from these patient studies, these reports suggest that, unlike tonic inhibition, enhanced $GABA_AR\alpha 1$-mediated phasic signalling in the repair phase may be beneficial for recovery. Furthermore, little is known about the overall changes in inhibitory signalling in cortical circuitry. For instance, it is unknown how stroke affects phasic GABA signalling in all the different cell types across the structurally organized layers of the somatosensory cortex. This information is crucial to understand the functional implication(s) of modified phasic GABA signalling. For example, modifying signalling in pyramidal layer 5 neurons, which provide the major output to subcortical structures, may have a different functional consequence than modifying layer 2/3 pyramidal neurons, which are primarily dedicated to cortico-cortical communication.

Given that $GABA_AR\alpha 1$ mediates the majority of phasic inhibition, and the recent clinical evidence for its potential role in brain repair, we used a combination of approaches to examine cortical layer- and cell-specific phasic GABA signalling in the repair phase of stroke and to determine the role of $GABA_AR\alpha 1$-mediated phasic inhibition in stroke

recovery. We focused on layer 5, the major output layer, and layer 2/3 as this is where Clarkson *et al.* (2010) observed effects on tonic GABA signalling after stroke. We used array tomography, a high-resolution imaging method (Micheva and Smith, 2007; Micheva *et al.*, 2010), to identify cortical layer-specific changes in $GABA_A$Rα1-containing synapse numbers after stroke. We performed intracellular whole-cell recordings to determine if the structural synaptic changes observed by array tomography were associated with a functional change in phasic $GABA_A$R inhibition and to identify which cell types undergo synaptic alterations. Last, we modulated $GABA_A$Rα1-mediated phasic inhibition to determine its effect on functional recovery. We provide the first evidence that phasic GABA signalling is increased in the peri-infarct cortex during the onset of post-stroke functional recovery. Furthermore, the increase in phasic GABA signalling is specific to layer 5. Lastly, we found, in contrast to tonic GABA signalling, that further enhancing phasic GABA signalling during the repair phase is beneficial for stroke recovery.

Materials and methods

See the online Supplementary material for further details. All animal procedures were approved by the Stanford University Administrative Panel on Laboratory Animal Care.

Stroke models

Animals were housed three to five per cage under a normal light/dark cycle. Adult (10–13 weeks old) male C57BL/6J mice (Jackson), weighing 25–30 g, were anaesthetized with isoflurane (2.5% in a mixture of 1 l/min of air and 0.2 l/min of oxygen). Core body temperature was measured by a rectal probe and maintained at 37°C throughout the surgery. Mortality rate was zero.

Distal middle cerebral artery occlusion model

The distal middle cerebral artery was exposed through a burr hole between the left eye and ear, cauterized, and cut just above the rhinal fissure. Sham animals only received the skin incision.

Photothrombotic model

After fixation in a stereotactic frame (David Kopf Instruments) the skull was exposed by midline incision of the skin. Rose Bengal (10 mg/ml in normal saline) was intraperitoneal injected (80 mg/kg). Five minutes later the exposed skull was illuminated (directly on the skull) for 15 min using a cold light source with an aperture of 2.4 mm, focused 0.0 mm anterior and 1.8 mm right of the Bregma.

Lesion size assessment

Tissue processing

For Day 2 post-stroke tissue, mice were sacrificed by deep anaesthesia and 2-mm thick coronal brain sections cut and stained with 2% triphenyltetrazolium chloride (TTC). For Days 7 and 28 post-stroke tissue, mice were perfused transcardially with heparinized phosphate-buffered saline (PBS) followed by 3% paraformaldehyde (PFA). Coronal sections were cut and 1 in every 16 sections (five sections per brain; 30 µm) was stained using the high-contrast silver stain method (Arac *et al.*, 2011) (Day 7 brains) or one in eight sections (eight sections per brain: 20 µm) were stained with Cresyl violet (Day 28 brains).

Lesion size measurement

Brain sections were scanned (Epson Expressions 10000XL flatbed scanner) and the total ipsilateral, contralateral and the infarct areas were measured in a blinded manner using ImageJ (NIH). Lesion size was calculated as: % lesion size = 100 × (total contralateral cortex area − healthy ipsilateral cortex area) / (total contralateral cortex area).

Array tomography

Array tomography was carried out as described (Micheva and Smith, 2007; Micheva *et al.*, 2010). Following perfusion with PFA the peri-infarct tissue was dissected out, ribbons of 30–35 serial ultrathin (70 nm) sections cut, stained for synaptic markers, and imaged. To analyse synapses in a similar brain region between animals, the following criteria were set (Supplementary Fig. 1A–C): (i) we defined the peri-infarct cortex as the cortical tissue within 0.8 mm from the medial edge of the lesion; (ii) synapses were analysed within the same cortical region, at + 0.26 to + 0.02 mm anterior to Bregma on sections that contained the anterior commissure; and (iii) only stroke-injured animals with lesions with a medial edge within 3.0 ± 0.3 mm from the midline were considered for analysis. The number of glutamatergic and GABAergic synapses, defined by the co-localization of pre- and postsynaptic markers (Table 1), was quantified using MATLAB.

Whole-cell patch-clamp electrophysiology

Whole-cell patch clamp recordings from acute neocortical brain slices were performed to evaluate GABA-mediated synaptic signalling in the peri-infarct cortex. Slice preparation and recordings were performed as described (Paz *et al.*, 2010, 2013), and done blinded to the experimental group for the stroke-injured animals treated with zolpidem versus vehicle. Spontaneous and miniature postsynaptic inhibitory current (IPSC) recordings were performed in the same neocortical region as the array tomography analysis (see above) and within ~800 µm from the edge of the lesion. Neocortical neurons were visually identified using differential contrast optics with a Zeiss (Oberkochen) Axioskop microscope and an infrared video camera. Recording electrodes made of borosilicate glass had a resistance of 2.5–6 MΩ when filled with intracellular solution (Supplementary material). Neurons were clamped at −70 mV and $GABA_A$ receptor-mediated spontaneous IPSC events were pharmacologically isolated by bath application of the ionotropic glutamate receptor blocker kynurenic acid (1 mM, Abcam); whereas miniature IPSCs were isolated using tetrodotoxin (0.5 µM TTX, Abcam) and kynurenic acid (1 mM, Abcam). At the end of the recordings,

Table 1 Classification of glutamatergic and GABAergic synapses based on the co-localization of pre- and post-synaptic markers

Synapse type	Presynaptic markers	Postsynaptic marker
Glutamate	Synapsin + (i) VGluT1; or (ii) VGluT2; or (iii) VGluT1 + VGluT2	PSD95
GABA	Synapsin + GAD + VGAT	$GABA_AR\alpha1$

Three glutamatergic subtypes (i–iii) were defined by the presence or absence of VGluT1 and VGluT2. As the majority of $GABA_A$ synapses contain $GABA_A$-Rα1 we chose this subunit as our GABA synapse postsynaptic marker. VGluT = vesicular glutamate transporter; $GABA_A$-Rα1 = α1 subunit of the GABA receptor; GAD = glutamate decarboxylase; VGAT = vesicular GABA transporter; PSD95 = postsynaptic density protein 95.

whole slices were fixed with PFA solution overnight and processed using immunofluorescent staining for biocytin and glial fibrillary acidic protein (Supplementary material). Firing pattern and cell morphology of the biocytin-labelled cells were used to distinguish pyramidal cells from fast-spiking interneurons. Access resistance was monitored in all the recordings, and cells were included for analysis only if the access resistance was <18 MΩ and the change of resistance was $<20\%$ over the course of the experiment. See Supplementary material for non-invasive membrane potential recordings.

In vivo drug administration

Zolpidem (Sigma-Aldrich) was dissolved in dimethylsulphoxide (DMSO) and then diluted 1:2 in 0.9% saline, to give a final concentration of 5 mM zolpidem (in 33% DMSO final). ALZET-1002 pumps containing zolpidem or vehicle (33% DMSO in 0.9% saline) were implanted subcutaneously at 3 days after stroke, under 2.0–2.5% isoflurane anaesthesia, and replaced every 2 weeks. The pumps delivered a zolpidem dose of 9.2 µg/24 h. Although detailed pharmacokinetic data for zolpidem are not available for mouse, based on the published information for rat (Garrigou-Gadenne *et al.*, 1989) we calculated that this dosing schedule results in subsedative blood levels (Benavides *et al.*, 1993; Vlainic and Pericic, 2010; Farkas *et al.*, 2013) of ~20 nM. In acute administration studies, 0.1 mg/kg or 1 mg/kg of zolpidem was administered by intraperitoneal injection at 1 h and 24 h post-stroke. No animals died after zolpidem treatment. One animal with a photothrombotic-induced lesion died after vehicle treatment; its data were excluded from analysis.

Behaviour analysis

The adhesive tape removal test was used to measure forepaw sensorimotor function (Bouet *et al.*, 2009) and the rotating beam test was used to measure more gross motor and sensory function (Cheng *et al.*, 2014). All behaviour testing was run during the light cycle in a blinded manner. For both tests mice were trained for 5 days prior to stroke surgery and a baseline recorded 1 day prior to stroke. Post-stroke mice were assessed at Day 2 and at Weeks 1, 2, 3 and 4. For the tape test, a small piece of adhesive tape (3 mm × 4 mm) was placed on each forepaw, and the time needed to contact and remove the tape from each forepaw was recorded. The test was stopped after 2 mins if the mice did not remove the tape in this time. Two runs were performed at each time point and the average score used in the analysis. Animals were randomized to the different groups based on their Day 2 (pretreatment score) such that the average and distribution of the scores was similar between the appropriate groups. Animals were excluded from the study if the time-to-contact at Day 2 post-stroke was <20 s as this indicated a minor stroke-related deficit that results in rapid spontaneous recovery to baseline within a few days. If animals did not complete the test on both the 'affected' and 'unaffected' paw after Day 2 post-stroke this was taken as a sign of lack of motivation rather than a sensorimotor deficit, and this trial was excluded from analysis. This was only observed at one time point in two vehicle-treated animals with the photothromobotic stroke. For the rotating beam test the mice were placed on a fibreglass beam (length 120 cm, diameter 13 mm) that rotated at 3 rpm. The distance travelled and the speed of traversing was obtained. Three trials were performed at each time point and the average of the fastest two speeds was used for analysis. Randomization of the animals was based on their tape test score, as this was our primary behaviour test. No test was run on Day 2 following photothrombotic-induced stroke as the animals were unable to stay on the beam at this time point.

Data acquisition and statistical analysis for electrophysiology

For data acquisition and analysis, we used a Digidata 1320 digitizer and pClamp9 (Molecular Devices). We amplified the signals with Multiclamp (Molecular Devices), and sampled and filtered them at 10 kHz. We detected and analysed spontaneous IPSCs with wDetecta, a custom postsynaptic current detection program (http://huguenardlab.stanford.edu/apps/wdetecta/). We detected and analysed miniature IPSCs with Mini Analysis Program (www.synaptosoft.com/MiniAnalysis). Numerical values are given as means ± SEM unless stated otherwise. For electrophysiology data tables (Supplementary Tables 1–5), we calculated average events per cell and compared all injured and non-injured cells by performing one-way ANOVA (parametric) or the Kruskal-Wallis one-way ANOVA on ranks (non-parametric). For cumulative probability distributions, each cohort population is composed by a random selection of 100 events from each cell (i.e. 1200 events from 12 cells) and compared all injured and non-injured event populations using the Kolmogoroff-Smirnoff test (non-parametric) to determine statistical significance ($P < 0.005$). We assessed normality and distribution equality using Kolmogorov-Smirnoff goodness-of-fit procedure and variance ratio test, respectively. We performed statistical analyses with Sigma Stat 3.5 and Origin 7.0 (Microcal Software). For IPSCs, we fitted the peak-to-baseline decay phase of the resulting current trace by a single exponential function.

Statistical analysis for array tomography and behavioural data

All values are expressed as mean ± SEM across animals, and data were analysed using GraphPad Prism software (v4.0c).

The normality of the data was confirmed by Kolmogorov-Smirnov test for each group. Tests for equal variance were done automatically by Prism as part of the statistical analysis; variances were not statistically different between groups being compared. For statistical analysis of the behaviour data, a repeated measures ANOVA was run on either the raw data (distal middle cerebral artery occlusion beam test) or log-transformed data (all other behaviour testing) followed by individual comparisons at each time point between vehicle- and zolpidem-treated stroked animals. All other data were analysed by either two-way ANOVA followed by Bonferroni *post hoc* test, one-way ANOVA followed by *post hoc* Tukey test, two-tailed Student's *t*-test, or two-tailed Mann Whitney test as indicated. P-values < 0.05 were considered statistically significant.

Results

Transient increase in $GABA_A$-Rα1-containing synapses specific to layer 5 peri-infarct cortex

To investigate the structural synaptic changes induced in layer 2/3 and layer 5a of the peri-infarct region, array tomography was used to quantify different synapse subtypes before and after stroke. Synapses were classified based on the co-localization of pre- and postsynaptic markers known to characterize the major subclasses of $GABA_A$ and glutamate synapses, as defined in Table 1 (Fig. 1A) (Neumann-Haefelin *et al.*, 1998; Redecker *et al.*, 2000). GABAergic synapse density significantly increased (~1.7-fold) at 1 week post-stroke in cortical layer 5a (Fig. 1B–D). The stroke-induced increase in detectable $GABA_A$-Rα1 containing synapses is layer-specific with a significant increase observed in layer 5a with no significant change observed in layer 2/3 (Fig. 1D). Furthermore, the increase in layer 5a was transient, observable at 1 week post-stroke but returning to baseline 1 month post-stroke (Fig. 1D). In contrast to GABA synapses, stroke had no observable effect on the density of the different glutamatergic synapse subclasses investigated either in layer 5 (Fig. 1C) or layer 2/3, at 1 week or at 1 month post-stroke (data not shown). Together, these data reveal that stroke-induced synaptic changes in the peri-infarct cortex can be dynamic, cortical layer-specific, and synapse class-specific.

Transient increase in $GABA_A$ signalling specific to layer 5 neurons

To determine if the transient and layer-specific increase in the number of $GABA_A$Rα1-containing synapses observed by array tomography was accompanied by a functional increase in phasic $GABA_A$ signalling, we examined spontaneous IPSCs in neurons from control and stroke-injured mice at 1 week and 1 month post-stroke. We performed whole-cell patch clamp recordings in the peri-infarct cortex from acute neocortical slice preparations. At 1 week post-stroke the average charge of spontaneous IPSCs in layer 5 pyramidal neurons was increased in stroke-injured mice (Fig. 2A–C and Supplementary Table 1). Cumulative probability plots of layer 5 pyramidal neuron spontaneous IPSC properties revealed a significantly higher proportion of the population with larger events present in the stroke-injured mice, indicated by the rightward shift of the charge curve at both low (<1000 fC) and high (1000–8000 fC) values (Fig. 2D). The increased charge of spontaneous IPSCs could reflect an increase in the number of receptors and/or an increase in spontaneous network activity. To determine if the increased charge is independent of changes in network activity we used TTX to block action potential firing and measured miniature IPSCs in these cells. We found an increase in the charge of miniature IPSCs from injured animals at 1 week post-stroke, which is consistent with a postsynaptic change in the number of GABAergic receptors (Supplementary Fig. 2). These results confirm that there is a functional increase in the postsynaptic response during phasic $GABA_A$ signalling. Interestingly, the conservative increase in charge of miniature IPSCs is insufficient to explain the relatively greater increase in spontaneous IPSC charge after stroke. This suggests that in addition to the increased postsynaptic GABA signalling observed with isolated miniature IPSCs, a separate as-yet unidentified activity-dependent mechanism(s) also contributes to the increase in phasic inhibition after stroke.

Stroke-injured animals also displayed an increase in mean spontaneous IPSC rise time (stroke: 1.10 ± 0.09 ms versus control: 0.88 ± 0.04 ms, $P = 0.04$; Supplementary Table 1), suggesting there is an increase in GABA signalling at more distal sites from the cell body in the injured mice. Consistent with the array tomography data, the increase in pyramidal neuron phasic $GABA_A$ signalling after stroke was cortical layer-specific as spontaneous IPSCs were not changed in layer 2/3 pyramidal neurons at 1 week post-stroke (Supplementary Table 1). Furthermore, the stroke-induced increase in layer 5 pyramidal neuron phasic signalling was transient, observed at 1 week but not at 1 month post-stroke (Fig. 2E and Supplementary Table 2).

Changes in GABA signalling were cell type-specific in layer 5. The aforementioned changes were observed in pyramidal cells while the major class of GABAergic inhibitory cells, fast-spiking interneurons, did not exhibit post-stroke changes in spontaneous IPSC amplitude, charge, or kinetics at 1 week post-stroke (Supplementary Table 1), although spontaneous IPSC frequency was increased (stroke: 3.50 ± 0.58 Hz versus control: 1.78 ± 0.27 Hz, $P = 0.04$; Supplementary Table 1). The increase in spontaneous IPSC frequency without concurrent increased spontaneous IPSC amplitude or charge in fast-spiking neurons of layer 5 suggests there are additional mechanisms contributing to an increase in phasic inhibition, such as increases in synapse number, presynaptic release probability, or axonal excitability (Hu and Jonas, 2014). The intrinsic excitability of the L5 pyramidal and fast-spiking neurons, which can also

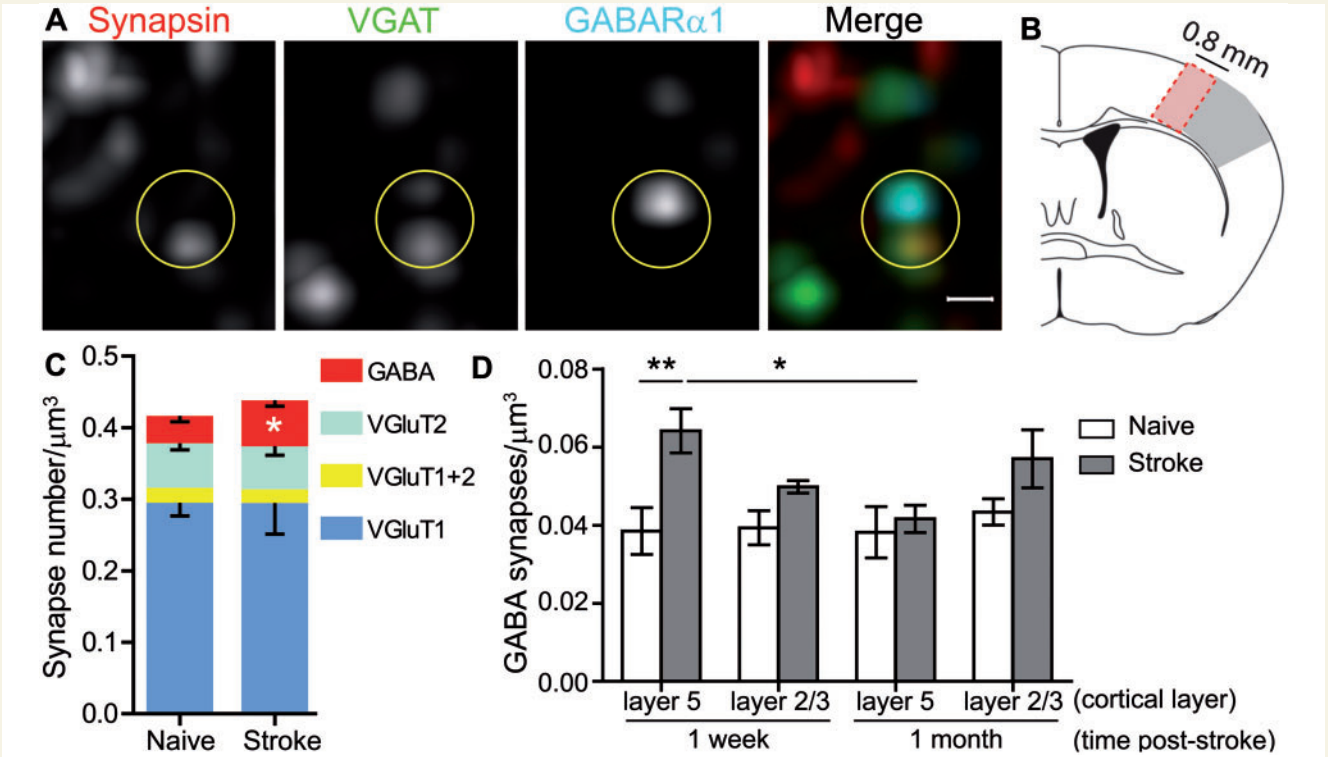

Figure 1 Stroke induces cortical layer-specific changes in GABA synapses. (**A**) Representative array tomography image for GABA synapses: synapsin (red), VGAT (green), $GABA_AR\alpha1$ (blue). Yellow circles mark triple co-localization. Co-localization with GAD is omitted for clarity. Scale = 200 nm. (**B**) Schematic illustrating the brain region used to analyse synapses. Grey indicates cortical lesion; red box indicates the peri-infarct cortical region taken for synapse analysis. (**C**) Array tomography quantification of GABA and glutamate synapse subtypes in layer 5a peri-infarct cortex at 1 week post-stroke reveals a significant increase in the number of GABA synapses. (**D**) Array tomography quantification of GABA synapses in different cortical layers and at different time points after stroke. For **C** and **D**, $n = 6$ animals per group at 1 week, $n = 5$ animals per group at 1 month. $^*P < 0.05$; $^{**}P < 0.01$ [*t*-test used in **C** and for layer 5 comparison in stroke animals (**D**); two-way ANOVA ($P = 0.0033$), with Bonferroni *post hoc* analysis, used for comparison of the four groups at 1 week in **D**]. Data shown as mean ± SEM.

affect the overall activity of the cells, was not different in the stroke-injured mice compared with the controls (Supplementary Tables 3 and 4).

An important factor affecting GABA-mediated inhibition is the chloride ion (Cl^-) concentration gradient, which determines the equilibrium potential (E_{GABA}) for inhibitory responses. Normally in the adult brain neuronal intracellular levels of Cl^- are low, resulting in inhibitory $GABA_A$ responses. However, during development, and after some injuries, intracellular levels of Cl^- increase so that $GABA_A$ responses can lose their efficacy in inhibiting neural function (reviewed in Kaila *et al.*, 2014). To determine if the E_{GABA} is altered after stroke, we used a non-invasive method relying on cell-attached recordings that avoided dialysis of intracellular Cl^- (Verheugen *et al.*, 1999). Using this method we measured the membrane potential in L5 pyramidal neurons in response to GABA puff application at 1 week post-stroke. We found that neither the resting potential nor the evoked GABA responses were affected in stroke-injured compared to control animals (Supplementary Fig. 3 and Supplementary Table 5) suggesting that E_{GABA} is not affected by the lesion.

Together, these results suggest that there is overall enhanced phasic GABA signalling in layer 5 of the peri-infarct neocortex at 1 week post-stroke. Furthermore, cortical layer- and cell-type specific postsynaptic changes in layer 5 pyramidal neurons return to basal levels by 1 month, which are consistent with the changes in GABA synapses observed by array tomography.

Post-stroke zolpidem treatment improves behavioural recovery

To determine what effect enhanced phasic GABA signalling during the repair phase might have on stroke recovery, animals were treated with a low (subsedative) dose of zolpidem, a $GABA_A$ positive allosteric modulator with high affinity for $\alpha1$-containing $GABA_A$ receptors (Crestani *et al.*, 2000). Zolpidem treatment was started on Day 3 post-stroke (i.e. subacute phase) (Fig. 3B). As the stroke lesion mainly affects the somatosensory cortex (Fig. 3A), the adhesive tape removal test was used to monitor functional recovery as it gives a measure of forelimb

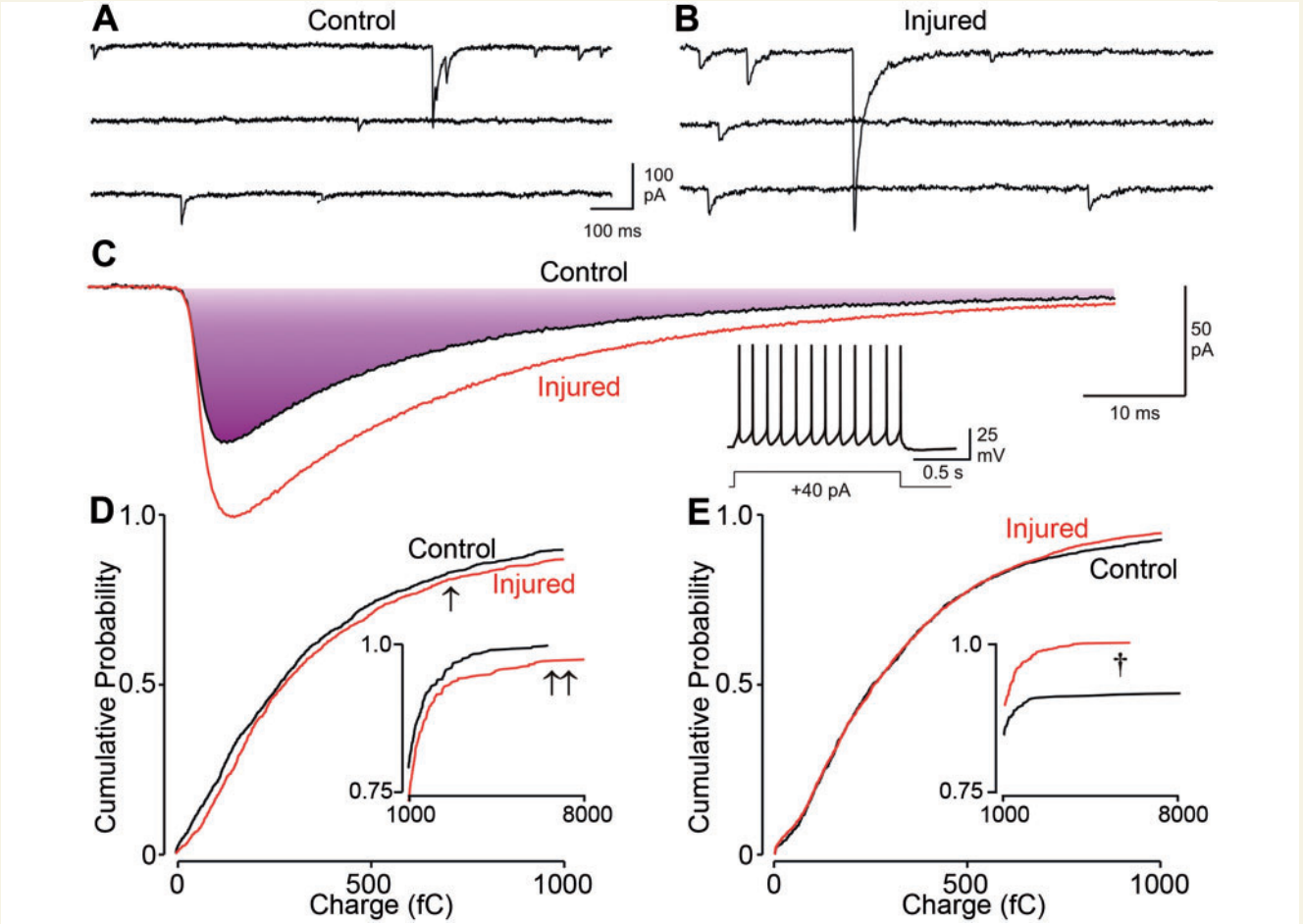

Figure 2 Stroke enhances postsynaptic inhibitory currents in layer 5 pyramidal neurons. (**A** and **B**) Spontaneous IPSC recordings from representative layer 5 pyramidal neurons from (**A**) control and (**B**) stroke-injured mice. (**C**) Ensemble-averaged IPSCs from the same pyramidal cells (control, black; injured, red). Spontaneous IPSC charge is calculated as the total area under the curve (purple). *Inset*: Action potential firing induced by an intracellular current injection in the pyramidal cell. Firing pattern was used to distinguish pyramidal cells from fast-spiking interneurons. (**D**) Cumulative probability histograms of isolated events at 1 week post-stroke from 10 slices from five control mice (n = 1500 events, 15 cells, 100 events per cell) and eight slices from five injured mice (n = 1100 events, 11 cells, 100 events per cell) reveal a higher proportion of events with larger charge present in the stroke-injured mice, demonstrated by the right shift of the charge curve at low values (charge < 1000 fC; indicated by single arrow) and the divergence of the charge curves especially at high values (*inset*: magnified portion of the plot between 1000–8000 fC; double arrow) (P = 0.005; Kolmogoroff-Smirnoff test). (**E**) Cumulative probability histograms of the charge of isolated events at 1 month post-stroke from nine slices from four control mice (n = 1300 events, 13 cells, 100 events per cell) and eight slices from four injured mice (n = 2300 events, 23 cells, 100 events per cell) are not different at low values (charge < 1000 fC; single arrow). *Inset* displays a leftward shift (not significant) at high values (charge 1000–8000 fC, indicated by the dagger) 1 week post-stroke (P = 0.08; Kolmogoroff-Smirnoff test).

sensorimotor function. Following stroke, the time taken for the animals to contact the adhesive tape on their affected (contralesional) forelimb increased (Fig. 3C); this deficit was maximal at 2 days post-stroke and recovered spontaneously to baseline within 1 month post-stroke. Chronic treatment with a low dose of zolpidem rapidly enhanced functional recovery ($P < 0.01$ by repeated measures ANOVA) with the effect observed as early as 4 days from treatment onset (i.e. 7 days post-stroke) (Fig. 3C). The time to remove the tape from the affected forelimb was similar in stroke-injured and control animals (Supplementary Fig. 4A); lack of a significant effect on this motor function aspect of the test is consistent with the motor cortex being largely intact. Use of the unaffected (ipsilesional) forelimb (Supplementary Fig. 4B and C) was unchanged by stroke or zolpidem treatment. In the rotating beam behaviour test, stroke caused a small but significant impairment in speed (P = 0.003, Day 0 versus Day 2). This deficit recovered to baseline by Day 14 in both groups and zolpidem treatment significantly enhanced the rate of recovery (Fig. 3D). Zolpidem treatment starting on Day 3 had no effect on lesion size at Day 7 post-stroke compared to vehicle-treated animals (vehicle group lesion size: 25.8% ± 6.1% of ipsilesional cortex; zolpidem group: 24.2% ± 4.8% of ipsilesional cortex). This is in contrast to treating animals with $GABA_A$ receptor agonists at stroke

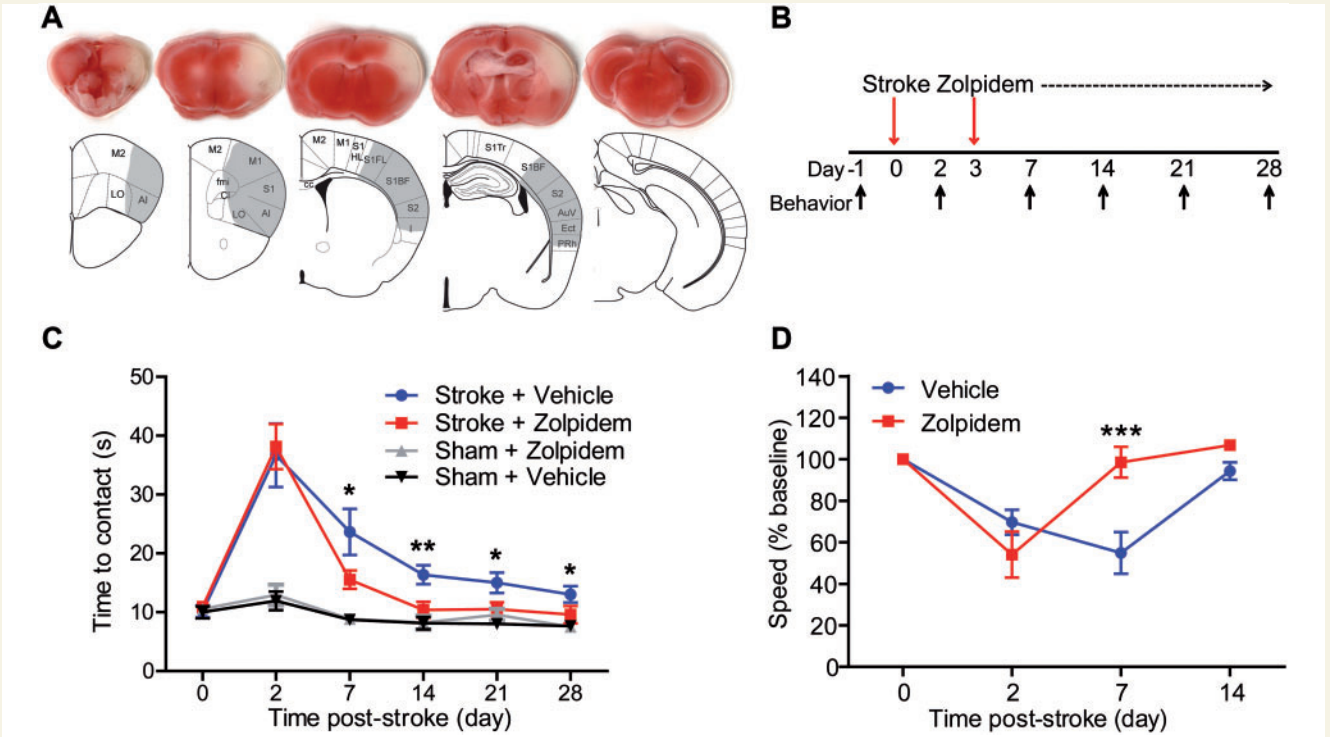

Figure 3 Zolpidem treatment enhances behavioural recovery after stroke. (**A**) A representative TTC-stained stroke-injured brain showing the lesion location (white: *upper panel*) mapped to the corresponding brain schematics (*lower panel*) taken from the Mouse Brain Atlas (Paxinos and Franklin, 2004) showing that the lesion (grey) is primarily in the somatosensory cortex (S1, S2). (**B**) Timeline indicating treatment paradigm. Short black arrows indicate behaviour testing days. (**C**) Zolpidem treatment starting at 3 days after distal middle cerebral artery occlusion-induced stroke enhanced functional recovery as assessed by the forelimb adhesive dot removal test. Pooled data from three experiments, each of which individually gave similar results; $n = 15$ (stroke/vehicle), $n = 16$ (stroke/zolpidem), and $n = 7$ (each sham group). Repeated measures two-way ANOVA ($P = 0.0072$). $^{*}P < 0.05$, $^{**}P < 0.01$ for stroke + vehicle versus stroke + zolpidem. (**D**) Zolpidem treatment enhanced the rate of recovery in the rotating beam test; $n = 5$ per group. Repeated measures two-way ANOVA ($P = 0.0499$). $^{***}P < 0.001$ by Bonferroni *post hoc* test. Data shown as mean ± SEM. AI = agran insular cortex; AuV = second auditory cortex; CC = corpus callosum; Cl = claustrum; Ect = ectorhinal cortex; fmi = forcepts minor corpus callosum; I = insular cortex; Lo = lateral orbital cortex; M1 = primary motor cortex; M2 = secondary motor cortex; Prh = perihinal cortex; S1 = primary somatosensory cortex; S1BF = S1 cortex, barrel field; S1FL = S1 cortex, forelimb; S1HL = S1 cortex, hindlimb; S1Tr = S1 cortex, trunk; S2 = secondary somatosensory cortex.

onset, which is known to decrease lesion size (Lyden and Hedges, 1992; Green *et al.*, 2000), and which we also observed when zolpidem was administered at stroke onset (Supplementary Fig. 5). These data indicate that enhancing phasic GABAergic signalling in the repair phase, starting 3 days after stroke, improves functional recovery without being neuroprotective.

We used a second stroke model, the photothrombotic model, to determine if the recovery-enhancing effects of zolpidem are complementary across different stroke models. In this model the lesion was primarily in the motor cortex (Fig. 4A), and resulted in much larger deficits in both the tape and beam tests than the previous stroke model (distal middle cerebral artery occlusion model) (Fig. 4B–D). In the tape test, stroke induced a significant deficit in the time to both contact and remove the tape from the affected limb (Fig. 4B and C). Animals treated with zolpidem exhibited a trend for improved recovery on both parameters. Zolpidem significantly enhanced the rate, but not extent, of recovery for tape contact, with greater recovery observed at Day 7 post-stroke in the zolpidem group; this differential recovery between the two groups dissipated at later time points. For tape removal, the effect of zolpidem was observed later with a trend for increased recovery seen from Days 14 to 28. In the rotating beam test, photothrombotic stroke caused a very large impairment of speed. Zolpidem had no effect on recovery (Fig. 4D), which may suggest that a certain threshold of innate (spontaneous) recovery is required for zolpidem to be effective. Zolpidem did not affect lesion size. Together, the data from the two stroke models show that zolpidem treatment in the repair phase of stroke can enhance recovery, with the most prominent effect being an accelerated rate of recovery.

Post-stroke zolpidem treatment enhances $GABA_A$ signalling

As zolpidem is a positive allosteric modulator it would further augment the stroke-induced increase in phasic

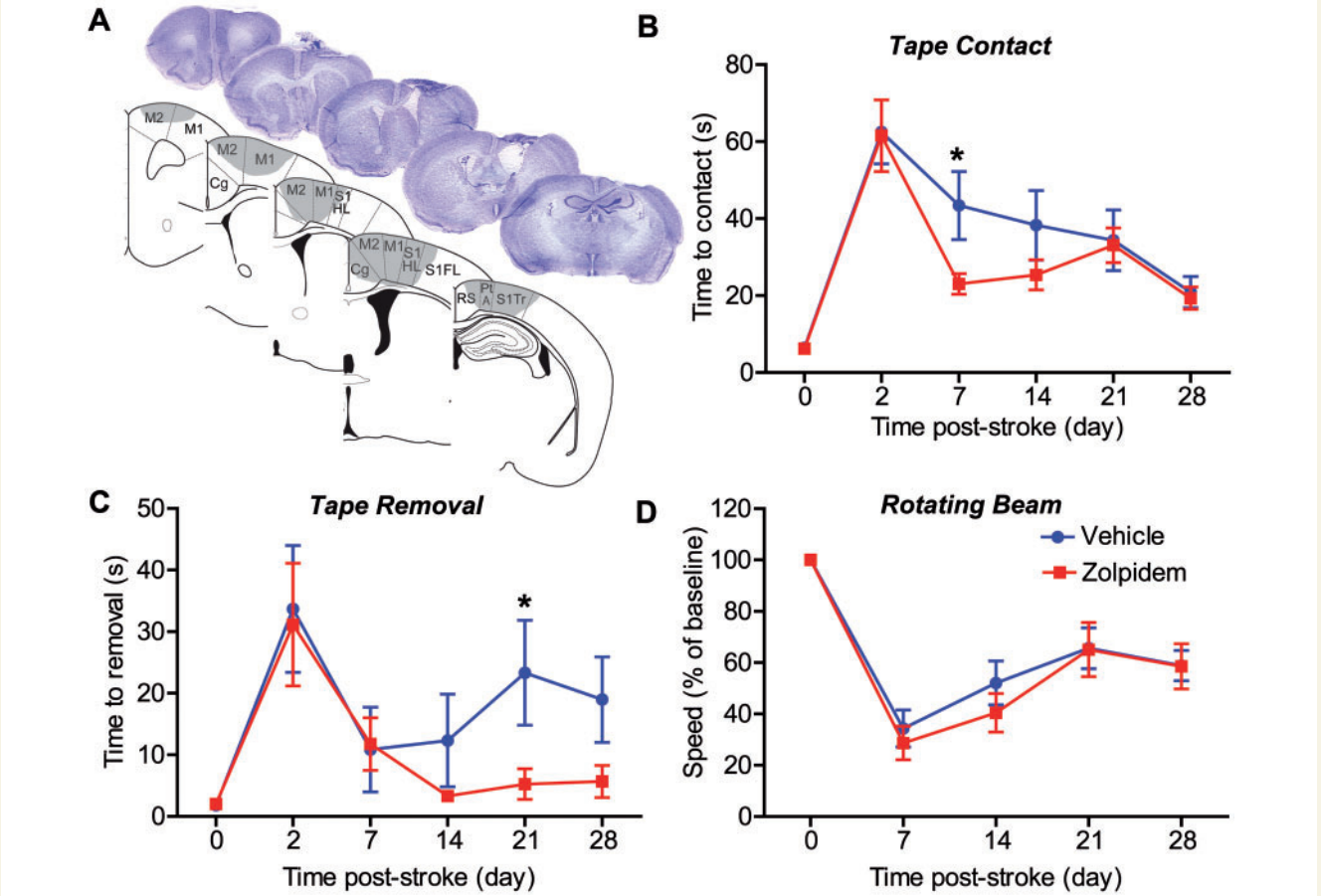

Figure 4 Effect of zolpidem treatment on recovery in a photothrombotic model of stroke. (**A**) Representative Cresyl violet-stained sections at 35 days post-stroke (*upper panel*) mapped to the corresponding brain schematics (*lower panel*) taken from the Mouse Brain Atlas (Paxinos and Franklin, 2004) showing that the lesion (grey) is primarily in the motor cortex (M1, M2). (**B–D**) Effect on recovery of zolpidem treatment starting at 3 days post-stroke as measured by (**B** and **C**) the adhesive tape test, and (**D**) the rotating beam test. Pooled data from four experiments, each of which individually gave similar results; $n = 17$ per group. $^*P < 0.05$ by two-tailed Mann–Whitney test. Data shown as mean ± SEM. Cg = cingulate cortex; M1 = primary motor cortex; M2 = secondary motor cortex; PtA = parietal association cortex; RS = retrosplenial cortex; S1FL = S1 cortex forelimb; S1HL = S1 cortex, hindlimb; S1Tr = S1 cortex, trunk.

inhibition we observed during the repair phase. However, this might lead to a compensatory downregulation in $GABA_A$Rs. Retention of full $GABA_A$R function under these conditions would support the hypothesis that the increase in phasic inhibition observed after stroke is beneficial to functional recovery. To address this issue we examined spontaneous IPSCs in layer 5 of the peri-infarct cortex at Day 7 post-stroke from animals treated with zolpidem or vehicle starting at 3 days post-stroke, and subjected to 1 week of behaviour testing. Brain slices were made from zolpidem- and vehicle-treated animals, and incubated in zolpidem-free artificial CSF for >2 h during spontaneous IPSC recording, removing any extracellular zolpidem. In zolpidem-treated animals, compared to the vehicle-treated group, spontaneous IPSCs exhibit increased frequency, amplitude and charge in layer 5 pyramidal neurons (Fig. 5) but not in fast-spiking interneurons (data not shown). Zolpidem-treatment did not alter the intrinsic excitability of pyramidal neurons or fast-spiking interneurons (Supplementary Table 6) suggesting that changes in spontaneous IPSC properties induced by zolpidem treatment are a result of changes in synaptic function rather than altered intrinsic excitability of neurons. In summary, our results indicate that the behavioural recovery induced by zolpidem treatment is associated with an enhanced phasic (synaptic) GABA signalling in excitatory pyramidal neurons but not in inhibitory neurons within layer 5 of the peri-infact area.

Discussion

Cortical circuit plasticity and remapping is important for functional recovery after stroke (Nudo *et al.*, 1996; Dijkhuizen *et al.*, 2001; Carmichael, 2006; Murphy and Corbett, 2009). Emerging evidence points to a role for GABA-mediated inhibition in modulating post-stroke plasticity as shown in a study where decreasing tonic (extrasynaptic) GABA inhibition in the repair phase of stroke, which starts days after stroke onset (Carmichael, 2006; Li

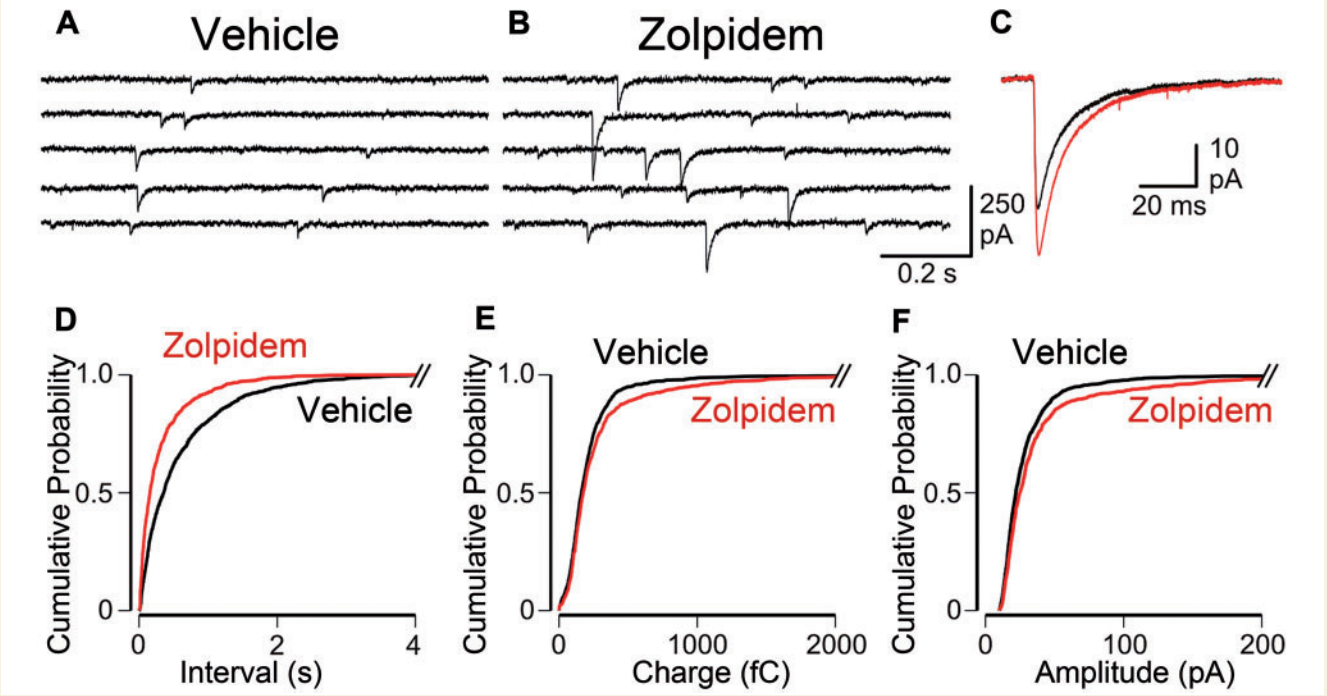

Figure 5 Zolpidem treatment enhances postsynaptic inhibitory currents in layer 5 pyramidal neurons. (**A** and **B**) Spontaneous IPSC recordings from representative layer 5 pyramidal neurons from stroke-injured mice treated with (**A**) vehicle and (**B**) zolpidem. (**C**) Ensemble-averaged spontaneous IPSCs from the same pyramidal cells (vehicle, black; zolpidem, red), plotted on the same timescale. (**D–F**) Cumulative probability histograms of isolated events from seven stroke-injured vehicle-treated mice (n = 1300 events, 13 cells, 100 events per cell) and six stroke-injured zolpidem-treated mice (n = 800 events, eight cells, 100 events per cell) demonstrate differences in frequency, charge and amplitude of the events (Frequency, $P = 10^{-24}$; Charge, $P = 10^{-6}$; Amplitude, $P = 10^{-8}$; Kolmogoroff-Smirnoff test).

et al., 2010), significantly improved functional recovery (Clarkson *et al.*, 2010). Much less is known about the role of phasic (synaptic) inhibition, a second mode of GABA signalling, in the repair phase of stroke. Our study provides the first structural and functional evidence of enhanced phasic GABAergic signalling in the peri-infarct cortex during the repair phase. Importantly, we demonstrate that boosting phasic GABA in the repair phase, using zolpidem, an FDA-approved positive allosteric GABA modulator, enhanced functional recovery without affecting lesion size. Thus, we identified a novel therapeutic strategy for stroke that targets plasticity-related recovery.

Phasic GABA signalling is driven by synaptic $GABA_AR$s (as opposed to extrasynaptic $GABA_AR$s that drive tonic signalling) (Farrant and Nusser, 2005). $GABA_AR$s containing the $\alpha1$ subunit are the most highly expressed $GABA_AR$ in the mammalian brain (Fritschy and Mohler, 1995) and mediate the majority of phasic inhibition. Using array tomography, a high resolution imaging method (Micheva and Smith, 2007; Micheva *et al.*, 2010) that overcomes the inherent difficulties of imaging synapses, we found a significant increase in the number of GABAergic synapses with $\alpha1$-subunit-containing receptors. This increase was cortical layer-specific—observed in layer 5 but not in layer 2/3—and transient, occurring during the onset of functional recovery and returning to baseline after 1 month. In contrast, we observed no change in the number of glutamatergic synapses. Previous published measurements of $GABA_AR$ protein expression suggested a decrease in the number of GABAergic synapses at a similar time point (Schiene *et al.*, 1996; Neumann-Haefelin *et al.*, 1998; Qu *et al.*, 1998; Redecker *et al.*, 2000; Jolkkonen *et al.*, 2003). These differences may be due to the various regions of interest and techniques used. Some studies used autoradiography measurements of ^{3}H-muscimol binding (a GABA agonist that binds at the same site as GABA) to assess $GABA_AR$ density (Schiene *et al.*, 1996; Qu *et al.*, 1998; Jolkkonen *et al.*, 2003). However, muscimol binding will reflect its distinct affinities for different $GABA_AR$ subtypes, and there is debate whether muscimol even binds to $\alpha1$ subunit receptors (Chandra *et al.*, 2010). Other studies used immunohistochemical analysis of different $GABA_AR$ subunits, including $\alpha1$, to assess $GABA_A$ receptor expression in individual cortical layers (Neumann-Haefelin *et al.*, 1998; Redecker *et al.*, 2000). However, this method measures global protein expression, which could mask what is occurring at the synapse. In contrast, array tomography enables quantitative measurements specifically at the level of the synapse.

Intracellular whole-cell recordings confirmed a functional increase in phasic $GABA_AR$-mediated signalling in the peri-infarct after stroke with the same temporal profile and cortical layer specificity observed for the aforementioned structural synaptic changes. We found that spontaneous

IPSCs were increased in layer 5 pyramidal neurons but not in layer 2/3 pyramidal neurons. These data suggest the postsynaptic properties of pyramidal neuron GABAergic synapses are enhanced after stroke. This was further corroborated by finding a stroke-induced increase in the charge of miniature IPSCs in layer 5 pyramidal neurons. Although $GABA_A$-R $\alpha1$ is known to be highly expressed in layer 5 fast-spiking interneurons (Bacci *et al.*, 2003), there was no change in the charge, amplitude, or kinetics of spontaneous IPSCs recorded from these cells. However, we observed an increase in frequency of layer 5 fast-spiking interneuron IPSCs. These observations suggest additional mechanism(s) enhance phasic GABAergic signalling in fast-spiking interneurons different from those that enhance GABAergic signalling in pyramidal neurons during the repair phase of stroke; these mechanisms remain to be elucidated. The individual consequences of these layer- and cell-specific changes in GABAergic inhibition on network activity, and the specific microcircuits affected, remain to be determined. Given that different populations of cells within different cortical layers have separate functions, it is likely that changes in $GABA_AR$ synapses onto distinct GABAergic interneurons and glutamatergic pyramidal cells will have diverse actions within local cortical circuits (Salin and Prince, 1996; Bacci *et al.*, 2003).

As layer 5 pyramidal neurons provide the major source of output from the cortex we anticipated that the post-stroke changes in phasic GABA activity onto these cells would affect post-stroke sensory and motor function. One might hypothesize that phasic GABA signalling, like tonic GABA, is detrimental to post-stroke plasticity and recovery (Schiene *et al.*, 1996; Neumann-Haefelin *et al.*, 1998; Qu *et al.*, 1998, Redecker *et al.*, 2000; Jolkkonen *et al.*, 2003). However, phasic GABA drives cortical plasticity and remapping in the neonatal and postnatal brain (Zheng and Knudsen, 2001; Derdikman *et al.*, 2003; Fagiolini *et al.*, 2004; Hensch and Stryker, 2004; Foeller *et al.*, 2005; Hensch, 2005; Mendez and Bacci, 2011; Lehmann *et al.*, 2012). As post-stroke brain repair processes may recapitulate developmental $GABA_AR$-mediated plasticity (Li *et al.*, 2010; Mendez and Bacci, 2011; Lehmann *et al.*, 2012), we speculated that phasic GABA activity could actually promote post-stroke plasticity-related recovery. Indeed, post-stroke increases in phasic GABAergic activity occur within the first week after stroke, which is when cortical map plasticity is thought to start in rodents (Carmichael, 2006; Li *et al.*, 2010). Moreover, we found that potentiating phasic GABA signalling during the repair phase, by treatment with a low dose of the $GABA_A$-R$\alpha1$ allosteric modulator zolpidem, significantly improved functional recovery in two models of stroke recovery. Of note, chronic treatment with zolpidem only enhanced phasic GABA signalling in layer 5 excitatory (pyramidal) neurons but had no effect on layer 5 inhibitory (fast-spiking) interneurons, suggesting treatment-induced plasticity is cell-type specific. Unlike GABA agonist treatment at stroke onset, which can be neuroprotective (Lyden and Hedges, 1992; Green *et al.*, 2000), our delayed zolpidem treatment paradigm, starting 3 days after stroke, did not affect lesion size. These data support the idea that enhanced phasic $GABA_A$-R$\alpha1$ signalling in the repair phase promotes plasticity-related recovery and presents a novel therapeutic strategy. Furthermore, our data identify zolpidem as a pharmacological agent to treat stroke. Zolpidem is an FDA-approved sleep aid, better known as Ambien, and therefore offers the potential of a tested and safe pharmacological agent to treat stroke. The low doses of zolpidem used in our study are below that required for sleep and do not induce drowsiness. Case studies show subsedative doses of zolpidem can improve motor and cognitive recovery after brain injury, including stroke (Cohen *et al.*, 2004; Shames and Ring, 2008; Hall *et al.*, 2010). This is often coincident with increased blood flow to the injured hemisphere after zolpidem treatment, suggestive of increased brain activity, and with desynchronized beta oscillations in the motor cortex, a known prerequisite for movement (Cohen *et al.*, 2004; Hall *et al.*, 2010). There are suggestions that the $\alpha1$ subunit specificity of zolpidem in this setting is an important component of its reparative function as other benzodiazepine site ligands do not have the same effect (Shames and Ring, 2008; Hall *et al.*, 2010). Our data have strong therapeutic implications as there are currently no FDA-approved drugs that target the brain repair phase of stroke or other CNS injuries.

Zolpidem binds with high affinity to the $\alpha1$ subunit and with 10-fold lower affinity to $\alpha2$ and $\alpha3$ subunits. Therefore, we cannot rule out the involvement of other $GABA_AR$ subunits in promoting recovery after stroke. Indeed, our electrophysiology data suggest that in addition to $GABA_ARs$ containing the $\alpha1$ subunit, $GABA_AR$'s containing other subunits also increase after stroke. $\alpha1$-containing $GABA_ARs$ have rapid decay kinetics; accordingly if only $\alpha1$-containing $GABA_ARs$ increased we would expect to see an increase in miniature or spontaneous IPSC amplitude with a decrease in duration. However, we observed an increase in charge with no significant change in amplitude and kinetics. These findings suggest changes in other $GABA_AR$ subunits after stroke, in addition to $\alpha1$, may contribute to the enhanced phasic GABA signalling. Identifying which additional subunits are altered and their potential involvement in functional recovery is an important focus for future studies.

A beneficial role of phasic GABA is in contrast to the detrimental role of tonic GABA signalling in post-stroke recovery (Clarkson *et al.*, 2010) and challenges the idea that enhanced GABA function is generally detrimental after stroke. This is not the first account of phasic and tonic inhibition mediating opposing outcomes. In absence epilepsy, agents that enhance tonic inhibition exacerbate seizures (Perucca *et al.*, 1998), while benzodiazepines that enhance phasic inhibition are effective antiepileptic drugs (Mikkelsen *et al.*, 1976; Huguenard and Prince, 1994). Our data offer a fresh perspective on GABA's role in brain repair after stroke. It also raises the intriguing question of why the brain activates two opposing actions in a

similar time frame. A balance between promoting and inhibiting plasticity is likely important to prevent maladaptive plasticity, which could induce stroke-related epilepsy, while still driving brain repair. The increase in phasic GABA signalling we observed is predominantly in cortical layer 5, the main source of cortical output, with very little effect seen in layer 2/3, the major source of interhemispheric cortico-cortical connections. Tonic GABA signalling, by contrast, is reported to be significantly altered in layer 2/3 (Clarkson *et al.*, 2010). This cortical layer specificity suggests that distinct cortical microcircuits respond differently after stroke. However, the significance of this and the interplay between phasic and tonic GABA in modulating stroke recovery remain to be determined. Moreover, as the $GABA_A$ receptors that mediate phasic and tonic inhibition differ in their subunit composition—phasic $GABA_ARs$ contain primarily α1-3,5 subunits whereas tonic $GABA_ARs$ contain primarily α4,6 subunits (Farrant and Nusser, 2005; Glykys *et al.*, 2008; Rudolph and Knoflach, 2011; Hines *et al.*, 2012)—it highlights the importance of targeted pharmacological intervention when considering therapeutic strategies for stroke that modulate GABA signalling.

In conclusion, our study provides the first account of increased phasic GABA activity in the early weeks following stroke injury and demonstrates that enhancing phasic GABA signalling in the repair phase with an FDA-approved drug promotes post-stroke functional recovery. Taken together our data offer new insights into mechanisms of brain repair and identify a novel therapeutic strategy and pharmacological target for stroke. Furthermore, our observations emphasize the necessity to distinguish the role of phasic and tonic GABA inhibition in stroke recovery as well as in normal brain functions.

Acknowledgements

We thank Dr Clarkson for helpful discussions about zolpidem, Drs Buckwalter, Cheng, and George for critical reading of the manuscript, Dr Alex Lee for writing a program to facilitate timing of the adhesive tape test, Cindy H. Samos for help editing the manuscript, and Elizabeth Hoyte for help with figure preparation. We also thank Isabel Parada for expert histology support. The monoclonal antibodies PSD-95 and $GABA_A$-Rα1 were developed by and/or obtained from the UC Davis/NIH NeuroMab Facility, supported by the National Institutes of Health (NIH) grant U24NS050606 and maintained by the Department of Neurobiology, Physiology and Behaviour, College of Biological Sciences, University of California, Davis, CA 95616.

Funding

The work was supported in part by NIH grant RO1 NS058784, Bernard and Ronni Lacroute, Russell and Elizabeth Siegelman, the Edward G. Hills Fund, and the William Randolph Hearst Foundation to G.K.S., and grants to T.H. from the Japan Society for the Promotion of Science, Uehara Memorial Foundation, KANAE Foundation for the Promotion of Medical Science, and the Nakayama Foundation for Human Science. J.T.P. is supported by the US National Institute of Neurological Disorders and Stroke (grant K99NS078118-01). J.R.H. is supported by grants from the US National Institute of Neurological Disorders and Stroke (5R01NS006477 and 5R01NS034774). Z.F. is supported by a graduate research fellowship from the National Science Foundation (DGE-114747). R.L. is a Senior Clinical Investigator of FWO Flanders.

Supplementary material

Supplementary material is available at *Brain* online.

References

Allen NB, Kaltenbach L, Goldstein LB, Olson DM, Smith EE, Peterson ED, et al. Regional variation in recommended treatments for ischemic stroke and TIA: Get with the Guidelines–Stroke 2003–2010. Stroke 2012; 43: 1858–64.

Arac A, Brownell SE, Rothbard JB, Chen C, Ko RM, Pereira MP, et al. Systemic augmentation of alphaB-crystallin provides therapeutic benefit twelve hours post-stroke onset via immune modulation. Proc Natl Acad Sci USA 2011; 108: 13287–92.

Bacci A, Rudolph U, Huguenard JR, Prince DA. Major differences in inhibitory synaptic transmission onto two neocortical interneuron subclasses. J Neurosci 2003; 23: 9664–74./

Benavides J, Peny B, Ruano D, Vitorica J, Scatton B. Comparative autoradiographic distribution of central omega (benzodiazepine) modulatory site subtypes with high, intermediate and low affinity for zolpidem and alpidem. Brain Res 1993; 604: 240–50.

Berkhemer OA, Fransen PS, Beumer D, van den Berg LA, Lingsma HF, Yoo AJ, et al. A randomized trial of intraarterial treatment for acute ischemic stroke. N Engl J Med 2015; 372: 11–20.

Bouet V, Boulouard M, Toutain J, Divoux D, Bernaudin M, Schumann-Bard P, et al. The adhesive removal test: a sensitive method to assess sensorimotor deficits in mice. Nat Protoc 2009; 4: 1560–4.

Carmichael ST. Cellular and molecular mechanisms of neural repair after stroke: making waves. Ann Neurol 2006; 59: 735–42.

Chandra D, Halonen LM, Linden AM, Procaccini C, Hellsten K, Homanics GE, et al. Prototypic GABA(A) receptor agonist muscimol acts preferentially through forebrain high-affinity binding sites. Neuropsychopharmacology 2010; 35: 999–1007.

Cheng MY, Wang EH, Woodson WJ, Wang S, Sun G, Lee AG, et al. Optogenetic neuronal stimulation promotes functional recovery after stroke. Proc Natl Acad Sci USA 2014; 111: 12913–8.

Clarkson AN, Huang BS, Macisaac SE, Mody I, Carmichael ST. Reducing excessive GABA-mediated tonic inhibition promotes functional recovery after stroke. Nature 2010; 468: 305–9.

Cohen L, Chaaban B, Habert MO. Transient improvement of aphasia with zolpidem. N Engl J Med 2004; 350: 949–50.

Crestani F, Martin JR, Mohler H, Rudolph U. Mechanism of action of the hypnotic zolpidem in vivo. Br J Pharmacol 2000; 131: 1251–4.

Derdikman D, Hildesheim R, Ahissar E, Arieli A, Grinvald A. Imaging spatiotemporal dynamics of surround inhibition in the barrels somatosensory cortex. J Neurosci 2003; 23: 3100–5.

Dijkhuizen RM, Ren J, Mandeville JB, Wu O, Ozdag FM, Moskowitz MA, et al. Functional magnetic resonance imaging of reorganization in rat brain after stroke. Proc Natl Acad Sci USA 2001; 98: 12766–71.

Fagiolini M, Fritschy JM, Low K, Mohler H, Rudolph U, Hensch TK. Specific $GABA_A$ circuits for visual cortical plasticity. Science 2004; 303: 1681–3.

Farkas RH, Unger EF, Temple R. Zolpidem and driving impairment–identifying persons at risk. N Engl J Med 2013; 369: 689–91.

Farrant M, Nusser Z. Variations on an inhibitory theme: phasic and tonic activation of GABA(A) receptors. Nat Rev Neurosci 2005; 6: 215–29.

Foeller E, Celikel T, Feldman DE. Inhibitory sharpening of receptive fields contributes to whisker map plasticity in rat somatosensory cortex. J Neurophysiol 2005; 94: 4387–400.

Fritschy JM, Mohler H. GABAA-receptor heterogeneity in the adult rat brain: differential regional and cellular distribution of seven major subunits. J Comp Neurol 1995; 359: 154–94.

Garrigou-Gadenne D, Burke JT, Durand A, Depoortere H, Thenot JP, Morselli PL. Pharmacokinetics, brain distribution and pharmaco-electrocorticographic profile of zolpidem, a new hypnotic, in the rat. J Pharmacol Exp Ther 1989; 248: 1283–8.

Glykys J, Mann EO, Mody I. Which GABA(A) receptor subunits are necessary for tonic inhibition in the hippocampus?. J Neurosci 2008; 28: 1421–6.

Green AR, Hainsworth AH, Jackson DM. GABA potentiation: a logical pharmacological approach for the treatment of acute ischaemic stroke. Neuropharmacology 2000; 39: 1483–94.

Hall SD, Yamawaki N, Fisher AE, Clauss RP, Woodhall GL, Stanford IM. GABA(A) alpha-1 subunit mediated desynchronization of elevated low frequency oscillations alleviates specific dysfunction in stroke–a case report. Clin Neurophysiol 2010; 121: 549–55.

Hensch TK. Critical period plasticity in local cortical circuits. Nat Rev Neurosci 2005; 6: 877–88.

Hensch TK, Stryker MP. Columnar architecture sculpted by GABA circuits in developing cat visual cortex. Science 2004; 303: 1678–81.

Hines RM, Davies PA, Moss SJ, Maguire J. Functional regulation of GABAA receptors in nervous system pathologies. Curr Opin Neurobiol 2012; 22: 552–8.

Hu H, Jonas P. A supercritical density of Na(+) channels ensures fast signaling in GABAergic interneuron axons. Nat Neurosci 2014; 17: 686–93.

Huguenard JR, Prince DA. Clonazepam suppresses GABAB-mediated inhibition in thalamic relay neurons through effects in nucleus reticularis. J Neurophysiol 1994; 71: 2576–81.

Jolkkonen J, Gallagher NP, Zilles K, Sivenius J. Behavioral deficits and recovery following transient focal cerebral ischemia in rats: glutamatergic and GABAergic receptor densities. Behav Brain Res 2003; 138: 187–200.

Kaila K, Price TJ, Payne JA, Mody I, Puskarjov M, Voipio J. Cation-chloride cotransporters in neuronal development, plasticity and disease. Nat Rev Neurosci 2014; 15: 637–54.

Lehmann K, Steinecke A, Bolz J. GABA through the ages: regulation of cortical function and plasticity by inhibitory interneurons. Neural Plast 2012; 2012: 892784.

Li S, Overman JJ, Katsman D, Kozlov SV, Donnelly CJ, Twiss JL, et al. An age-related sprouting transcriptome provides molecular control of axonal sprouting after stroke. Nat Neurosci 2010; 13: 1496–504.

Lyden PD, Hedges B. Protective effect of synaptic inhibition during cerebral ischemia in rats and rabbits. Stroke 1992; 23: 1463–9; discussion 9–70.

Mendez P, Bacci A. Assortment of GABAergic plasticity in the cortical interneuron melting pot. Neural Plast 2011; 2011: 976856.

Micheva KD, Busse B, Weiler NC, O'Rourke N, Smith SJ. Single-synapse analysis of a diverse synapse population: proteomic imaging methods and markers. Neuron 2010; 68: 639–53.

Micheva KD, Smith SJ. Array tomography: a new tool for imaging the molecular architecture and ultrastructure of neural circuits. Neuron 2007; 55: 25–36.

Mikkelsen B, Birket-Smith E, Bradt S, Holm P, Bparm, Lung M, et al. Clonazepam in the treatment of epilepsy. A controlled clinical trial in simple absences, bilateral massive epileptic myoclonus, and atonic seizures. Arch Neurol 1976; 33: 322–5.

Mittmann T, Qu M, Zilles K, Luhmann HJ. Long-term cellular dysfunction after focal cerebral ischemia: in vitro analyses. Neuroscience 1998; 85: 15–27.

Murphy TH, Corbett D. Plasticity during stroke recovery: from synapse to behaviour. Nat Rev Neurosci 2009; 10: 861–72.

Neumann-Haefelin T, Hagemann G, Witte OW. Cellular correlates of neuronal hyperexcitability in the vicinity of photochemically induced cortical infarcts in rats in vitro. Neurosci Lett 1995; 193: 101–4.

Neumann-Haefelin T, Staiger JF, Redecker C, Zilles K, Fritschy JM, Mohler H, et al. Immunohistochemical evidence for dysregulation of the GABAergic system ipsilateral to photochemically induced cortical infarcts in rats. Neuroscience 1998; 87: 871–9.

Nudo RJ, Wise BM, SiFuentes F, Milliken GW. Neural substrates for the effects of rehabilitative training on motor recovery after ischemic infarct. Science 1996; 272: 1791–4.

Paxinos G, Franklin KBJ. The mouse brain in stereotaxic coordinates. San Diego: Academic Press; 2004.

Paz JT, Christian CA, Parada I, Prince DA, Huguenard JR. Focal cortical infarcts alter intrinsic excitability and synaptic excitation in the reticular thalamic nucleus. J Neurosci 2010; 30: 5465–79.

Paz JT, Davidson TJ, Frechette ES, Delord B, Parada I, Peng K, et al. Closed-loop optogenetic control of thalamus as a tool for interrupting seizures after cortical injury. Nat Neurosci 2013; 16: 64–70.

Perucca E, Gram L, Avanzini G, Dulac O. Antiepileptic drugs as a cause of worsening seizures. Epilepsia 1998; 39: 5–17.

Qu M, Buchkremer-Ratzmann I, Schiene K, Schroeter M, Witte OW, Zilles K. Bihemispheric reduction of GABAA receptor binding following focal cortical photothrombotic lesions in the rat brain. Brain Res 1998; 813: 374–80.

Redecker C, Luhmann HJ, Hagemann G, Fritschy JM, Witte OW. Differential downregulation of GABAA receptor subunits in widespread brain regions in the freeze-lesion model of focal cortical malformations. J Neurosci 2000; 20: 5045–53.

Rudolph U, Knoflach F. Beyond classical benzodiazepines: novel therapeutic potential of GABAA receptor subtypes. Nat Rev Drug Discov 2011; 10: 685–97.

Salin PA, Prince DA. Electrophysiological mapping of GABAA receptor-mediated inhibition in adult rat somatosensory cortex. J Neurophysiol 1996; 75: 1589–600.

Schiene K, Bruehl C, Zilles K, Qu M, Hagemann G, Kraemer M, et al. Neuronal hyperexcitability and reduction of GABAA-receptor expression in the surround of cerebral photothrombosis. J Cereb Blood Flow Metab 1996; 16: 906–14.

Shames JL, Ring H. Transient reversal of anoxic brain injury-related minimally conscious state after zolpidem administration: a case report. Arch Phys Med Rehabil 2008; 89: 386–8.

Verheugen JA, Fricker D, Miles R. Noninvasive measurements of the membrane potential and GABAergic action in hippocampal interneurons. J Neurosci 1999; 19: 2546–55.

Vlainic J, Pericic D. Zolpidem is a potent anticonvulsant in adult and aged mice. Brain Res 2010; 1310: 181–8.

Zheng W, Knudsen EI. Gabaergic inhibition antagonizes adaptive adjustment of the owl's auditory space map during the initial phase of plasticity. J Neurosci 2001; 21: 4356–65.